Desalination and Water Treatment
www.deswater.com
doi: 10.1080/19443994.2013.808588

52 (2014) 5611–5628
August

Taylor & Francis
Taylor & Francis Group

Regenerable hydrogels based on poly(acrylic acid-sodium acrylate-acrylamide) modified by sodium humate for high removal of Pb^{2+} and Fe^{2+} ions: metal adsorption kinetics and thermodynamic studies

Tripti Singh, Reena Singhal*

Department of Plastic Technology, Harcourt Butler Technological Institute, Kanpur, UP 208002, India
Email: reena_singhal123@rediffmail.com

Received 8 February 2013; Accepted 16 May 2013

ABSTRACT

A novel superabsorbent hydrogel based on poly(acrylic acid-sodium acrylate-acrylamide)/sodium humate poly(AAc-SA-AM)/SH was applied as adsorbent to adsorb metal ions (Pb^{2+}, Fe^{2+}) from the aqueous solutions. The factors affecting adsorption capacity of the poly(AAc-SA-AM)/SH hydrogel such as contact time, pH, temperature, SH content (wt.%), initial concentration of the metal ion, and ionic strength were systematically investigated. Results from the experimental data revealed that an appropriate addition of SH (2.44 wt.%) not only increases the metal ion adsorption of poly(AAc-SA-AM) hydrogel but also improves its regeneration ability. The results showed that the adsorption equilibrium data fitted the Langmuir isotherm better than the Freundlich isotherm. The maximum binding capacity for Pb^{2+} ion was 198 and 164 mg/g/l for Fe^{2+} ion for per g of poly(AAc-SA-AM)/SH (SH_4) hydrogel (high as compared to many other adsorbents). The changes in thermodynamic parameters were also calculated, and the negative ΔG° and ΔH° confirmed that the adsorption process was spontaneous and exothermic. The kinetic studies revealed that the adsorption process can be well described by the pseudo-second-order kinetic model.

Keywords: Hydrogels; Metal ion adsorption; Adsorption kinetics; Thermodynamic parameter

1. Introduction

The tremendous increase in the use of metal ions over the past few decades has posed a threat to the environment and human health (including diarrhea, liver damage, anemia, and dark urine) even at low concentrations [1]. Strict legislation on the discharge of toxic metal ions like Cd, Fe, Cu, Pb, etc. makes it necessary to develop various efficient separation and preconcentration treatment methods for the removal of pollutants from wastewater [2]. Lead, a highly toxic metal ion causes respiratory problems, memory loss, difficulties during pregnancy, nerve disorders, reproductive disorders, digestive problems, etc. Iron may cause choroiditis, conjunctivitis, and retinitis if it remains in contact with the tissues. Chronic inhalation of excessive amount of iron oxide fumes or dust may result in growth of a benign pneumoconiosis called siderosis that is observable as an X-ray change. Inhalation of excessive amount of iron oxide may increase the risk

---

*Corresponding author.

1944-3994/1944-3986

of lung cancer in workers exposed to pulmonary carcinogens. The commonly used traditional separation and preconcentration methods for the treatment of metal-contaminated wastewater include filtration, chemical precipitation, chelating ion exchange, liquid–liquid extraction, reverse osmosis, electrochemical treatment, neutralization, and adsorption [3,4]. However, in comparison with the other processes for the treatment of polluted aqueous effluents, the adsorption process is considered to be a highly efficient, economical, regenerable, and promising method for treating metal-contaminated waste water [5,6].

In recent years, a variety of the adsorbents introduced for the removal of metal ions from aqueous solutions. Hydrogel is a three-dimensional macromolecular network made up of a polymer backbone, water, and a cross-linker to form a complex network structure of high molecular weight. The most important property of hydrogels is their capability to swell in the presence of water and shrink in the absence of it. Superabsorbent hydrogels (SAHs) form one special class of hydrogels with the capacity to absorb huge amounts of water, and the absorbed water is hardly removable even under pressure. Due to their superior properties (more hydrophilicity, high swelling capacity, and biocompatibility) compared to traditional absorbents (such as cotton, pulp, and sponge, etc.), SAHs are widely used in many products, such as hygiene products (sanitary napkins, disposable diapers, and surgical pads, etc.), [7] and in medicine for drug delivery systems [8,9]. In addition to health care products, they are used in soil for some agricultural and horticultural programs [10], water-blocking tapes, sealing material, gel actuators, drilling fluid additives [11], communication cables, and antiredecomposition agents for detergent formulations, where water absorbency and water retention are essential.

Few researchers have modified SAHs in order to enhance their water absorbency, absorption rate, and gel strength [12,13]. Hydrogel shows the ability to shrink and swell in response to change in external stimuli, such as solvent, ionic strength, pH, temperature, pressure, and electric and magnetic fields [14,15]. Existence of these properties encourage the use of SAHs and make them promising for water purification. Acrylic acid was chosen due to its low cost, responsivity on external stimuli (i.e. shows response behavior towards change in external swelling medium condition), and presence of carboxylic group, which makes it a good chelating agent as well as highly hydrophilic. Polyacrylamide and copolymers of polyacrylamide have high hydrophilicity. The amide group of acrylamide acts as a good trapping and binding agent for various metal ions. Acrylic acid was partially neutralized to sodium acrylate to convert the carboxylic group into carboxylate group. The binding of metal ions with SAHs (i.e. adsorption of metal ions onto SAHs) depends on the interaction between the negatively charged functional group and the cations via ion exchange. Sodium acrylate (anionic in nature) consists of carboxylate functional groups and so the interaction between the cations and carboxylate ions occur directly and fastly, so the cations will easily attach to carboxylate group and thus increases the adsorption rate.

Most of the SAHs used in practice are primarily pure synthetic polymers having high production cost, low stability, and poor environment-friendly characteristics. To overcome these drawbacks, the development of hydrogel, with the incorporation of abundantly available natural raw materials including the ones that are low-cost, nontoxic, renewable, and biodegradable in nature such as humic acid or humates, has been focused upon. Humic acid is an important material, which can be found in many places in nature and it is a principal component of humic substances. It is composed of multifunctional aliphatic components and aromatic constituents and contains large number of functional hydrophilic groups (such as carboxylates and phenolic hydroxyls) [16]. It contains quinine structure, bound and free phenolic –OH groups, oxygen and nitrogen as bridge units, and $-NH_2$ and –COOH groups differently placed on aromatic ring. Due to presence of these carboxylate and phenolate groups, sodium humate forms complexes/chelates with metal ions.

It was reported that the presence of humates/humic acid can be beneficial for the adsorption of metal ions. Recently, humic acid/humates were introduced into the hydrogel to enhance their equilibrium swelling [17]. Li et al. [18] prepared polyacrylamide–polyacrylic acid superabsorbent and studied its binding capacity for various metal ions under varying conditions of pH, time, ionic strength, and initial metal ion concentration. Hizal et al. [19] observed that in the presence of humic acid, clay mineral behaved more like a chelating agent for metal ion adsorption than a simple ion exchanger, as in the presence of humic acid the stability of surface complexes was higher in comparison to binary metal ion complexes. Zhen Yi et al. [20] synthesized sodium humate/poly(*N*-isopropylacrylamide) hydrogels and examined its swelling and decoloring properties and concluded that SH enhances the adsorption of methylene blue dye.

In the present study, we have synthesized a novel biodegradable multifunctional superabsorbent hydrogel based on acrylic acid, sodium acrylate, and acrylamide monomers modified with sodium humate; as a combination of natural and synthetic polymers;

applied it for the adsorption of Pb^{2+} and Fe^{2+} ions. To the best of our knowledge, the reports on adsorption of Pb^{2+} and Fe^{2+} ions using poly(AAc-SA-AM)/SH hydrogel has not been reported. The effects of different experimental parameters such as pH, contact time, SH concentration, ionic strength, and initial Pb^{2+}ions and Fe^{2+}ions concentration on the adsorption process were investigated to optimize the adsorption conditions. Models fit to equilibrium adsorption isotherm and kinetic data were evaluated here to understand the adsorption process and its mechanism to validate the usefulness of this novel hydrogel in the field of wastewater treatment. Thermodynamic parameters for the adsorption process of Pb^{2+} and Fe^{2+} ions were also investigated. Fourier transform infrared spectroscopy was done to elucidate the mechanism of Pb^{2+} and Fe^{2+} ions adsorption onto hydrogel surface. The desorption capacity and reusability of the solid adsorbent were assessed based on five consecutive adsorption–desorption cycles.

2. Experimental

2.1. Materials

Acrylic acid ((AAc), analytical grade), acrylamide ((AM), analytical grade), ammonium persulfate ((APS), analytical grade), sodium hydroxide ((NaOH), analytical grade), *N*,*N*-methylene bisacrylamide ((NMBA), analytical grade), lead (II) nitrate (analytical grade), and ferrous (II) sulfate (analytical grade) were purchased from CDH New Delhi, India. Methanol (analytical grade) was purchased from Qualikems, New Delhi. Acrylamide was recrystallized from methanol before use. Sodium humate ((SH), analytical grade) (supplied from Aldrich) was used as received. Double distilled water was used throughout the experiments.

2.2. Synthesis of poly(AAc/AM/SH) hydrogels

The chemical structure and digital photo of poly (AAc-SA-AM)/SH hydrogel are shown in Fig. 1. The synthesis of poly(AAc-SA-AM)/SH hydrogel can be

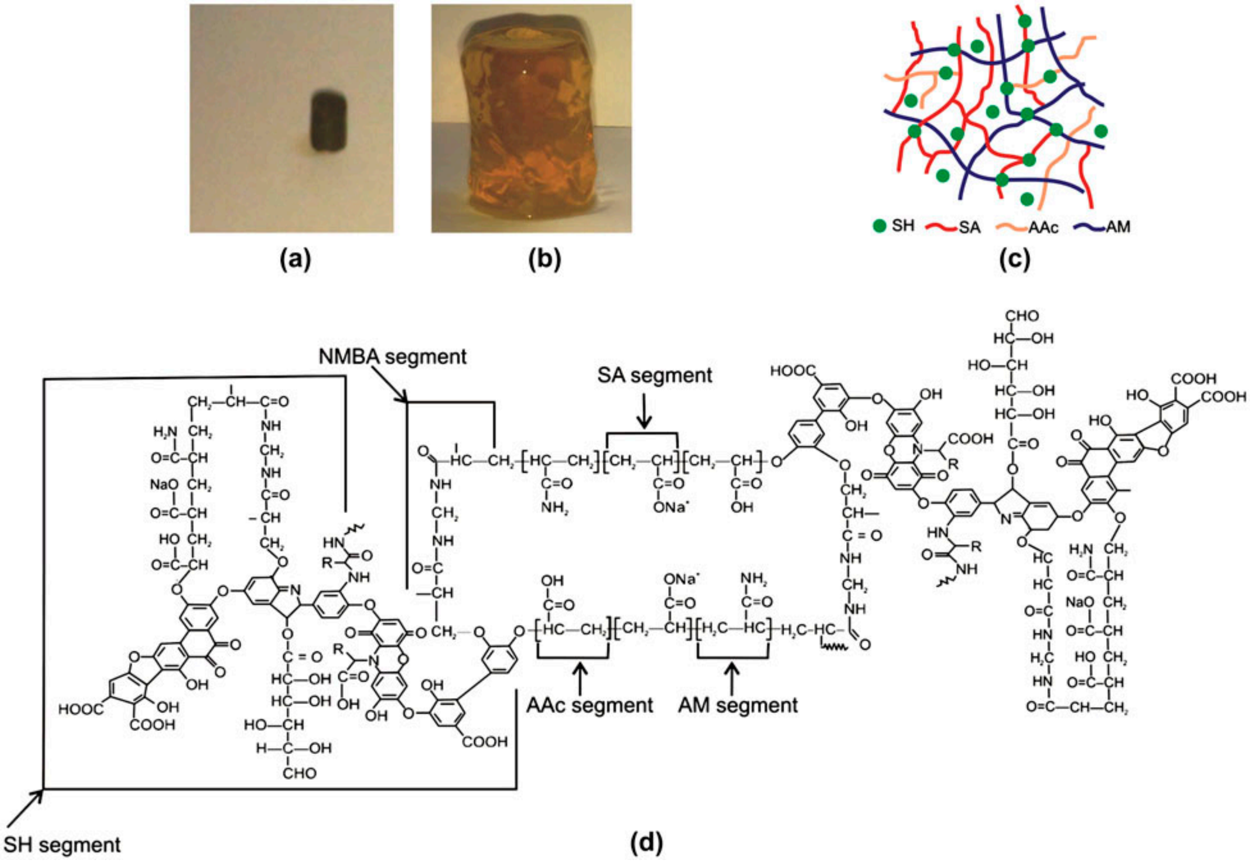

Fig. 1. (a) digital photo of poly(AAc-SA-AM)/SH superabsorbent hydrogel, (b) poly(AAc-SA-AM)/SH superabsorbent hydrogel after adsorption of Fe (II) ion, (c) Schematic structure of poly(AAc-SA-AM)/SH superabsorbent hydrogel, and (d) Possible chemical structure of poly(AAc-SA-AM)/SH superabsorbent hydrogel.

described as- AM (5 gm) was dissolved in 10 ml distilled water. 5 g of AAc was taken in a beaker and neutralized with NaOH solution. Amount of NaOH required for the neutralization of AAc to a partial neutralization degree of 75% was taken and dissolved in 20 ml distilled water. NaOH solution was added drop by drop to AAc under constant stirring, and then partially neutralized AAc/SA was obtained. AAc/SA was then added to AM solution under constant stirring. After that, the reaction mixture was taken in a 250 ml three-neck round-bottom flask. The NMBA (0.20 wt.% of total monomer) was added to the monomer solution and then appropriate quantity of SH was dispersed into mixed solution. The reaction mixture was stirred with nitrogen for 30 min. Then, the mixed solution was heated in a thermostat oil bath at 60℃ gradually and after that the initiator, APS (0.40 wt.% of total monomer), was introduced. The solution was stirred vigorously and a nitrogen atmosphere was maintained until the gel was formed. After polymerization, the reaction product was removed and cut into small pieces, washed with methanol and water, and then dried in an oven at 60° C until the weight of the product was constant.

The actual feed compositions are provided in Table 1

2.3. Fourier transforms infrared spectroscopy (FT-IR) studies

The FT-IR spectra of poly(AAc-SA-AM)/SH (SH_4) hydrogel before and after metal ion adsorption were recorded with Perkin-Elmer Spectrophotometer using solid pellet potassium bromide (KBr) after completely drying the sample at 60℃ up to constant weight.

2.4. Scanning electron microscopy

The surface morphology of poly(AAc-SA-AM)/SH (SH_4) hydrogel before and after metal ion adsorption was examined under scanning electron microscope (SEM). Dried hydrogels were coated with a thin layer of pure gold in S150 Sputer Coater and imaged in a SEM (LEO Electron Microscopy Ltd. England).

2.5. Measurement of Pb^{2+}/ Fe^{2+} ions adsorption

To study the adsorption of metal ions, 50 mg of dry hydrogel was introduced in 100 ml of Pb^{2+} ions salt solution and Fe^{2+} ions salt solution and was left in solution at different constant temperatures (±0.5℃) for 48 h. The initial pH of the Pb^{2+}/ Fe^{2+} ions solution was adjusted by using 0.1 mol/l HCl or 0.1 mol/l NaOH solutions. The samples were withdrawn at predetermined time intervals (1, 2, 3, 4, 5, 6, 7, 8, 9, 10, 11, 12, and 24 h), and then 2 ml of solution was sampled to analyze Pb^{2+} ions and Fe^{2+}ions content left in solution by UV–vis spectroscopy.

The analysis of adsorption capacities of the poly (AAc-SA-AM)/SH hydrogel for Pb^{2+}/ Fe^{2+} ions were performed through the following equation:

$$q_e = \frac{C_o - C_e}{m} \times V \tag{1}$$

where q_e is the amount of Pb^{2+}/Fe^{2+} ions adsorbed at equilibrium, C_o is the initial concentration of Pb^{2+}/ Fe^{2+} ions, and C_e is the equilibrium concentration of Pb^{2+}/Fe^{2+} ions; V is the volume of the Pb^{2+}/Fe^{2+} ions solution; and m is the mass of hydrogel sample.

Table 1

The feed compositions for synthesis of various poly(AAc-SA-AM)/SH hydrogels and their adsorption and desorption capacity; Pb^{2+}ion and Fe^{2+}ion after repeated adsorption–desorption cycle

Sample designation	AAc (wt.%)	SA (wt.%)	AM (wt.%)	SH (wt.%)	Adsorption capacity				Desorption capacity			
					Pb^{2+}		Fe^{2+}		Pb^{2+}		Fe^{2+}	
					A_1	A_5	A_1	A_5	D_1	D_5	D_1	D_5
SH_1	12.50	37.50	50.00	00.00	148.00	146.82	110.00	109.30	97.30	97.90	93.20	93.40
SH_2	12.40	37.22	49.62	0.74	162.00	161.75	132.00	130.10	98.50	97.80	93.60	92.90
SH_3	12.34	37.03	49.38	1.23	178.00	177.48	151.00	149.81	98.40	98.50	94.10	94.76
SH_4	12.20	36.58	48.78	2.44	198.00	197.52	164.00	163.47	97.10	95.80	91.80	91.90
SH_5	12.05	36.14	48.19	3.61	157.00	154.99	143.00	141.70	96.00	96.70	89.40	89.40
SH_6	11.62	34.88	46.51	6.98	131.00	130.10	98.00	96.29	95.80	93.05	87.40	85.70

Other conditions: NMBA, 0.20 wt.%; APS, 0.40 wt.%; distilled water, 30 ml; temperature 60 ℃.A_1-adsorption amount in first cycle (mg/g), A_5-adsorption amount in fifth cycle (mg/g).D_1-desorption(%) in first cycle, D_1-desorption(%) in fifth cycle.

In order to evaluate the influence of temperature on adsorption capacity for Pb^{2+}/Fe^{2+} ions, isotherms were established at 30, 45, and 60°C.

For the kinetic study, adsorption experiments were conducted as follows: 50 mg of adsorbent was suspended in 100 ml solution containing 1,000 mg/l of Pb^{2+}/Fe^{2+} ions. The pH of solution was adjusted with 0.1 mol/l HCl or 0.1 mol/l NaOH solutions. Then, the sealed flasks were put in a shaker bath at 30 ± 0.5°C. The flasks were then taken out at different times for the analysis of Pb^{2+}/Fe^{2+} ions concentrations. The rate of Pb^{2+}/Fe^{2+} ions adsorption was evaluated from the amount of Pb^{2+}/Fe^{2+} ions adsorbed at different times.

To evaluate the influence of pH on Pb^{2+}/Fe^{2+} ions adsorption, experiments were performed at different initial pH, ranging between 1.0 and 12.0. An initial phosphate ion concentration of 1,000 mg/L and 50 mg of adsorbent were used. The solutions were shaken for 48 h at 30 ± 0.5°C.

2.6. Desorption and regeneration

Elution of Pb^{2+}/Fe^{2+} ions from the poly(AAc-SA-AM)/SH hydrogel was carried out in 25 ml of 0.1 M HNO_3 solution (elution medium) for 24 h at temperature 30 ± 0.5°C. The hydrogel-adsorbed Pb^{2+}/Fe^{2+} ions were placed in the elution medium and stirred with a magnetic stirrer at room temperature. The superabsorbent hydrogel was washed several times with distilled water and methanol and then dried at 60°C for 24 h. The regenerated hydrogel was employed for another adsorption. The final Pb^{2+}/Fe^{2+} ions concentration in the aqueous phase was determined by UV–vis spectroscopy. Desorption ratio was calculated from the amount of Pb^{2+}/Fe^{2+} ions adsorbed on the polymer surface and final Pb^{2+}/Fe^{2+} ions concentration in the elution medium.

Desorption ratio was calculated using the following expression:

$$\text{Desorption ratio } = \frac{\text{Amount of } Pb^{2+}/Fe^{2+}\text{ions desorbed to the elution medium}}{\text{Amount of } Pb^{2+}/Fe^{2+}\text{ions adsorbed on the superabsorbent hydrogel}} \times 100 \qquad (2)$$

In order to determine the reusability of the superbsorbent hydrogels, consecutive adsorption–desorption cycle was repeated for the five times of the same sample.

3. Result and discussion

3.1. Characterization of poly(AAc-SA-AM)/SH hydrogel

3.1.1. FT-IR studies

The FT-IR spectra of representative sample poly (AAc-SA-AM)/SH hydrogel (SH_4) before (metal ions free hydrogel) and after metal ion adsorption (hydrogel with adsorbed metal ions) were investigated and shown in Fig. 2. Few facts are readily apparent from the figure, such as the presence of a broad band at 3,402 cm^{-1} (Fig. 2(a)), which was broadened and appeared at 3,392 cm^{-1} (for Pb^{2+} ions) and at 3,390 cm^{-1} (for Fe^{2+} ions) after adsorption due to interaction of Pb^{2+} and Fe^{2+} ions with $–NH_2$ or –OH groups. Also, the FT-IR spectra of metal-loaded poly(AAc-SA-AM)/SH hydrogel showed that the absorption band at 1,715 cm^{-1} (due to C=O group of carboxyl group) was obviously weakened after the adsorption and shifted to lower wave number; 1,695 cm^{-1} (for Pb^{2+} ions) and 1,691 cm^{-1} (for Fe^{2+} ions) after adsorption. The absorption band at 1,278 cm^{-1} (due to aromatic ether) does not appear after the adsorption. In addition, the absorption band at 1,560 cm^{-1}(corresponding to symmetric stretching of the carboxylate) was shifted to 1,520 cm^{-1}(for Pb^{2+} ions) and 1,517 cm^{-1} (for Fe^{2+} ions), and the band at 1,400 cm^{-1} (corresponding to asymmetric stretching of the carboxylate) was shifted to 1,480 cm^{-1}(for Pb^{2+} ions) and 1,481 cm^{-1} (for Fe^{2+} ions). On the basis of FT-IR analysis of unloaded and metal ion-loaded poly(AAc-SA-AM)/SH hydrogel, it can be concluded that $–NH_2$, –OH, COO^-, and COOH groups are possibly involved in metal ion adsorption onto the poly(AAc-SA-AM)/SH hydrogel.

3.1.2. SEM

The SEM images of poly(AAc-SA-AM)/SH hydrogel (SH_4) before and after the metal ion adsorption are shown in Fig. 3. It can be observed from the Fig. 3(a) that the structure of SH_4 hydrogel prior to metal ion adsorption is highly porous. Fig. 3(b) and 3(c) shows the SEM of the sample SH_4 after the Pb^{2+} and Fe^{2+} ion adsorption (after 48 h adsorption), respectively. It is obvious from the Fig. 3(b) and (c) that Pb^{2+} and Fe^{2+} ions adsorption blocks the open

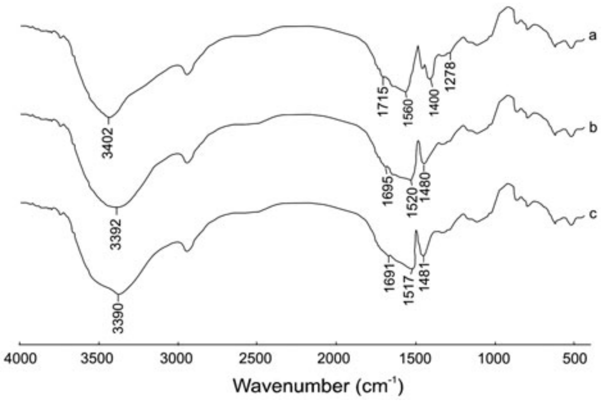

Fig. 2. FT-IR spectra of (a) poly(AAc-SA-AM)/SH (SH_4) superabsorbent hydrogel, (b) poly(AAc-SA-AM)/SH (SH_4) superabsorbent hydrogel after swelling in Pb(II) ions solution, and (c) poly(AAc-SA-AM)/SH (SH_4) superabsorbent hydrogel after swelling in Fe(II) ions solution.

pores of hydrogel. The adsorption of Pb^{2+} and Fe^{2+} ions onto the SH_4 hydrogel leads to the formation of a nonporous and smooth wave surface morphology, which is due to newly formed layer of metal ions on the hydrogel surface. These evidences clearly reveal that metal ions have a prominent effect on the structure of poly(AAc-SA-AM)/SH hydrogel (SH_4) surface by sealing the pores.

3.2. Adsorption mechanism

For the adsorption field, the chief challenge is to clearly identify the adsorption mechanism. In the case of superabsorbent hydrogel and metal ions, interaction is assumed to be because of electrostatic forces and coordinate bonds. In this study, the Pb^{2+} and Fe^{2+} ions adsorption on to the adsorption surface mainly occurs through the ion exchange and chelation between positively charged metal ions and phenolic hydroxylics as well as carboxylate groups.

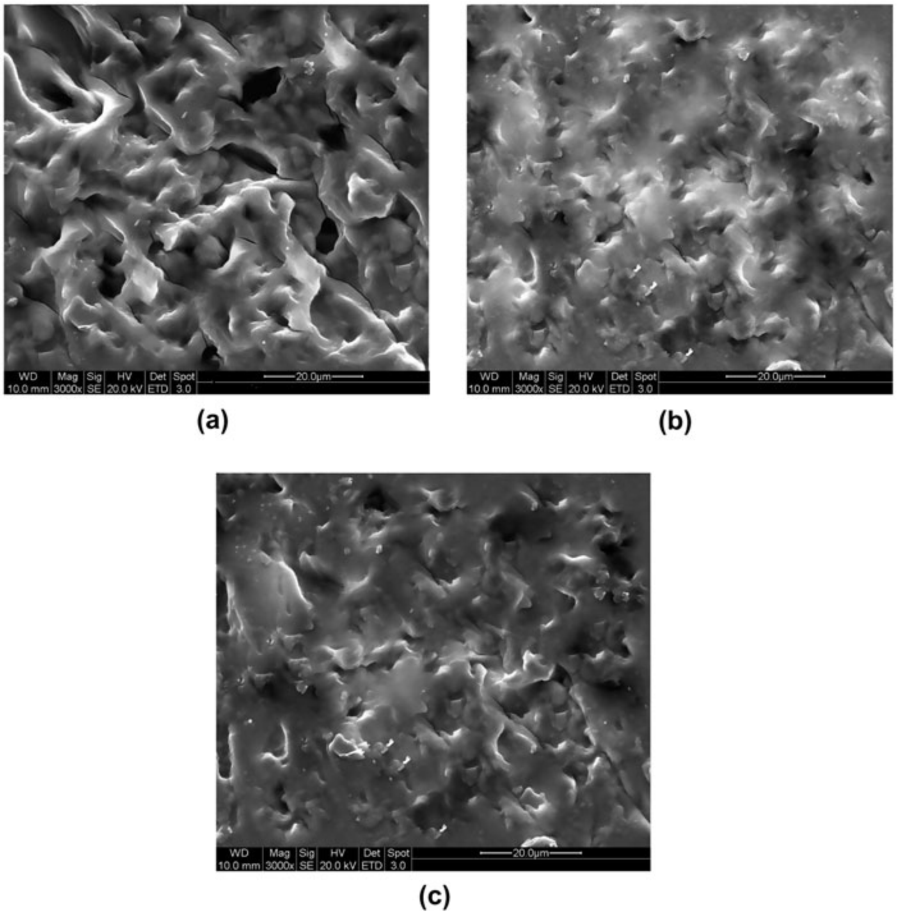

Fig. 3. (a) SEM of poly(AAc-SA-AM)/SH (SH_4) superabsorbent hydrogel, (b) SEM of poly(AAc-SA-AM)/SH (SH_4) superabsorbent hydrogel after swelling in Pb(II) ions solution, and (c) SEM of poly(AAc-SA-AM)/SH (SH_4) superabsorbent hydrogel after swelling in Fe(II) ions solution.

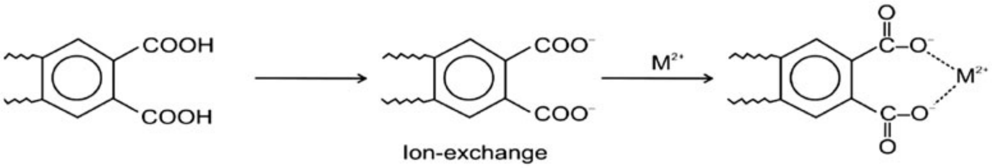

(3)

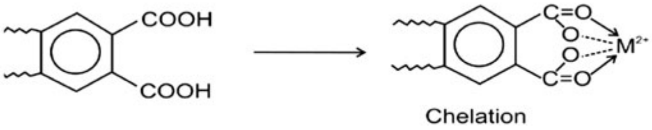

(4)

The adsorption mechanism can be depicted by the following facts: (i) firstly, to understand the adsorption mechanism of $Pb^{2+}$and Fe^{2+}ions adsorption onto poly(AAc-SA-AM)/SH hydrogel, the FT-IR spectra of representative sample, SH_4 hydrogel, before (metal ions free hydrogel) and after adsorption (hydrogel with adsorbed metal ions) were investigated (discussed in section characterization of poly(AAc-SA-AM)/SH hydrogel). (ii) pH variation of metal ion solution at the equilibrium; during the adsorption process, as the equilibrium achieved the pH value decreased. This can be attributed due to the fact that the poly(AAc-SA-AM)/SH hydrogel has many –COOH and –OH groups, which function as the adsorption sites for metal ion exchange and chelation. These functional groups in the aqueous solutions dissociate to yield protons and decrease the pH of solution. That is testified by the change in pH of the suspension before and after the adsorption. All these findings suggest that the groups, $–NH_2$, $–COO^-$, and –COOH, were involved in adsorption mechanism. On considering the above discussion, it can be concluded that chelation and ion exchange coexist during the adsorption process Fig. 4.

3.3. Effect of pH of solution on adsorption

The pH of solution is one of the most important parameters influencing the adsorption amount of metal ions. It can affect the solution chemistry of the metal ions (e.g. complexation and hydrolysis), as well as the protonation of the functional groups on the adsorbents [21]. In this study, metal ion removal was examined at various pH values for hydrogels SH_1 and SH_4. Fig. 5(a) shows variation of adsorption capacity with respect to various pH values for Pb^{2+} ions (between pH 2.00–7.0) and Fe^{2+} ions (between pH 1–3). The poly(AAc-SA-AM)/SH hydrogel is an anionic polymer due to presence of acidic functional group. Protonation and deprotonation of these acidic groups are influenced by variation in the pH values. As can be observed from the Fig. 5(a), the metal ion uptake was found to increase with an increase in pH and then increased slowly until it was constant. After that, on further increasing the pH it slightly lowered down. These results can be interpreted as follows: at low pH, on the one hand, there can be strong competition between hydrogen ions and metal ions for the adsorption sites, which made the availability of metal cations to activated adsorption sites difficult to take place; on

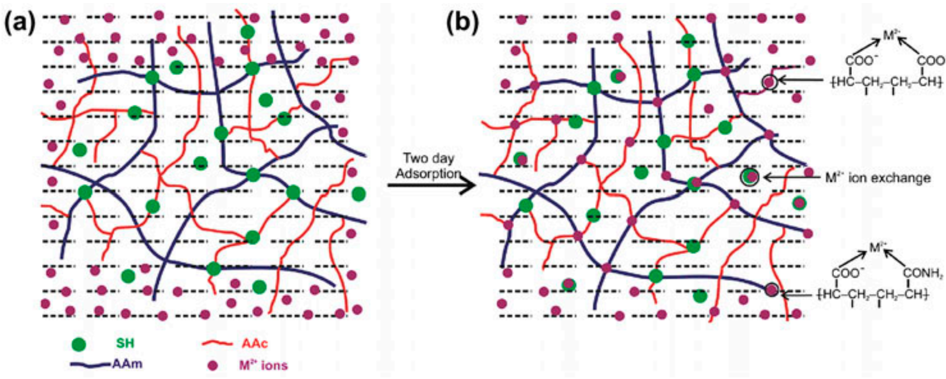

Fig. 4. Schematic representation of metal ion adsorption onto superabsorbent hydrogel poly(AAc-SA-AM)/SH (a) before metal ion adsorption and (b) after metal ion adsorption.

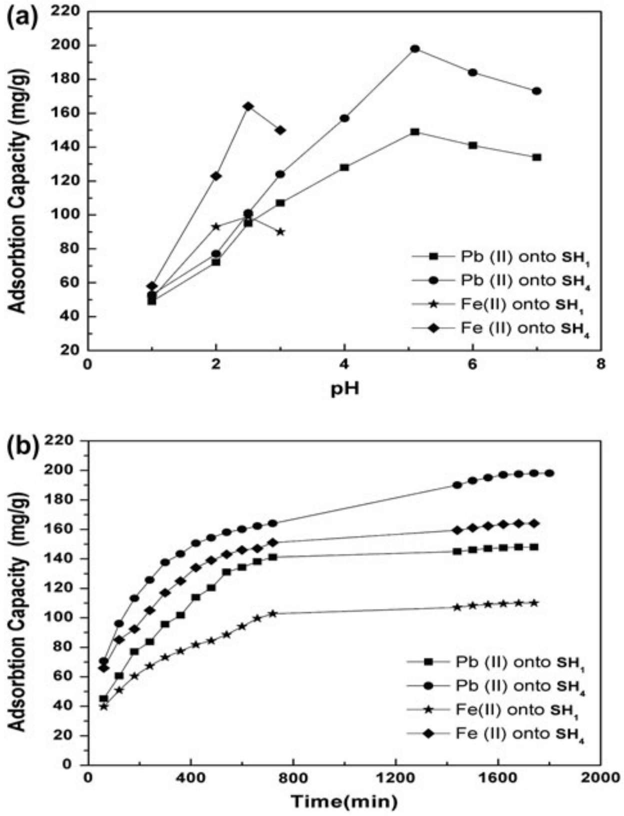

Fig. 5. Effect of pH and contact time on the adsorption of Pb^{2+}ions and Fe^{2+}ions, (a) Effect of pH and (b) Effect of contact time. Hydrogel-SH_4, contact time, 48 h; initial ion concentration, 1,000 mg/L; temperature 30 ± 0.5˚C; and hydrogel content, 50 mg.

the other hand, the COO^- ions present in the polymeric matrix are converted to their protonated form that may hinder the interaction of poly(AAc-SA-AM)/SH hydrogel with metal ion, so the adsorption capacities for the metal ions decreases. Conversely, at the higher pH, most of the -COOH groups are ionized; thereby making a higher number of ionized carboxylic groups available. Therefore, there is an increase in the interaction between metal cations and carboxylate groups, resulting in an increase in metal ion adsorption. The above results revealed that the maximum adsorption capacities for the metal ions were obtained at pH 5.1 for Pb^{2+}, and at 2.5 for Fe^{2+} ions. For Pb^{2+}, the pH of 5.55 was selected as the initial pH value to avoid the production of precipitation in the aqueous solution. For the Fe^{2+} ion, the adsorption experiments could not be done at pH higher than 3 because of the insolubility of metal hydroxide. The maximum removal capacities at optimum pH are 198 mg/g and 164 mg/g for Pb^{2+} and Fe^{2+} ions, respectively.

3.4. Effect of contact time on adsorption of Pb^{2+}/ Fe^{2+} ions

In order to investigate the effect of contact time on the adsorption of Pb^{2+}/Fe^{2+} ions on SH_4 SAHs from aqueous solution, the adsorbents were equilibrated with adsorbate solution for predetermined period, as shown in Fig. 5(b). As clear from Fig. 5(b), the amount of Pb^{2+} and Fe^{2+} ions adsorbed onto poly(AAc-SA-AM)/SH hydrogel (SH_4)was higher than the amount adsorbed by poly(AAc-SA-AM) hydrogel (SH_1). Since poly(AAc-SA-AM)/SH hydrogel possesses more number of negatively charged functional groups than poly (AAc-SA-AM) hydrogel and the capability of SH to trap the metallic cations has long been known, this result was expectable. It appears that attractive interaction may be the most important factor in adsorption process. It can also be observed that the adsorption capacity of hydrogel for both Pb^{2+}/Fe^{2+} ions increased with the increase of contact time from 60 to 360 min. of adsorption. More than 85% of the equilibrium adsorption capacity occurred within 660 min. and 480 min. for Pb^{2+} and Fe^{2+} ions, respectively. The high

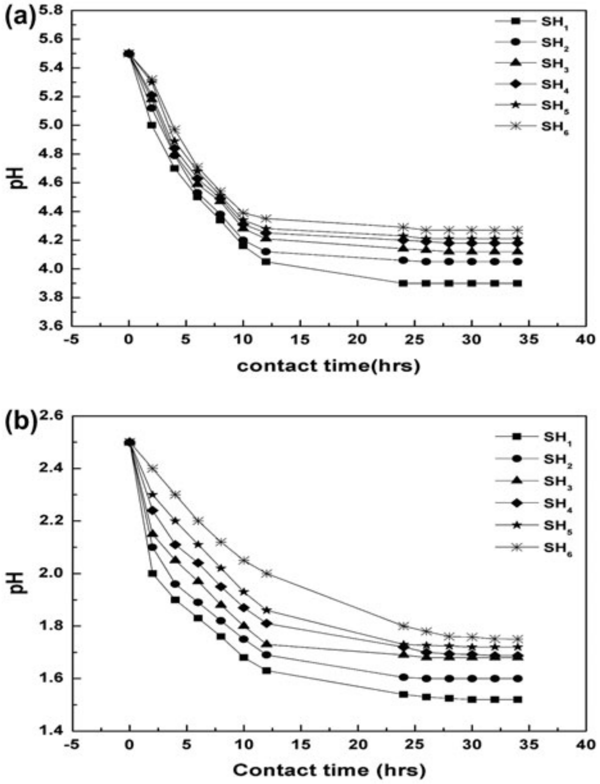

Fig. 6. Variation of pH value of the metal ions suspension solution with contact time: (a) Variation of pH value of Pb^{2+} ions suspension solution with contact time (b) Variation of pH value of Fe^{2+} ions suspension solution with contact time.

initial adsorption rate can be explained as: initially, adsorption sites were void and so metal ions can easily interact with these binding sites. For both ions, the uptake almost remained constant after 1,560 min., and with prolonged time, the adsorption amount hardly increased, so 1,560 min. could be considered as the contact time for the adsorption under our experimental conditions.

Fig. 6(a) and (b) showed the pH variation of the Pb^{2+} and Fe^{2+} ions solutions with change in contact time during adsorption process. It can be examined that pH of solutions decreased rapidly when contact time increased from 1 to 10 h. and then decreased quite little. As the adsorption equilibrium was set up, the pH values of the solutions did not change any more. It is well known that SH consists of many negatively charged groups [16] which may promote the adsorption of protons on the poly(AAc-SA-AM)/SH hydrogel and result in rise of pH value of the final solutions [20]. But, the result was different. This phenomenon can be explained by the following equations (Eq. (5) and (6)):

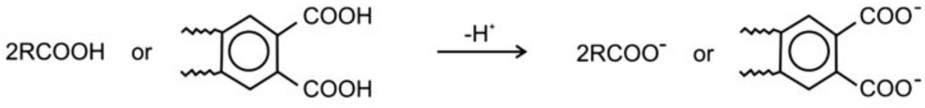

(5)

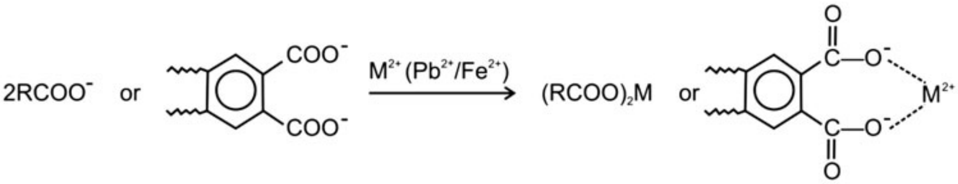

(6)

It is known that poly(AAc-SA-AM)/SH hydrogel is three-dimensional cross-linked polymer network and its network is composed of lots of carboxyl groups, which may be served as the adsorption sites for chelation and ion exchange. In aqueous solution, these groups on the polymer network dissociate and become ionized (Eq. (5)). The functional group –COOH dissociates in presence of metal ions and is converted to carboxylate ions and releases the protons in solution. These carboxylate ions bond with Pb^{2+}/Fe^{2+} ions to form a neutral species and equilibrium is established as the contact time increases, i.e. (the reaction proceeded to equilibrium) the dissociation of –COOH group (i.e. ion exchange and chelation) increases. More dissociation of functional groups means more release of protons to solution. As the concentration of protons in solution increases, the pH of the solution goes down. So, it can be concluded that pH of solution decreases with increase of contact time. In addition to this, the pH variation of solutions with the contact time suggests that bothchelation and ion exchange regulate the adsorption process.

3.5. Effect of SH concentration on adsorption of Pb^{2+}/ Fe^{2+} ions

Effect of SH content on adsorption capacity of poly (AAc-SA-AM)/SH hydrogel for Pb^{2+}(pH 5.1; initial concentration 1,000 mg/l; temperature 303.15 K) and Fe^{2+} (pH 2.5; initial concentration 1,000 mg/l; temperature 303.15 K) ions has been shown in Fig. 7(a) and (b), respectively. It can be observed from the both figures that under the same conditions, the removal capacities of poly(AAc-SA-AM)/SH hydrogel with different concentrations of SH are different. Poly(AAc-SA-AM)/SH hydrogel shows higher removal capacity than that of poly(AAc-SA-AM) hydrogel. It can also be seen that the adsorption capacity of poly(AAc-SA-AM)/SH hydrogel increases from 149 to 198 mg/g and from 110 to 164 mg/g for Pb^{2+} ions and Fe^{2+} ions, respectively, when the SH content was less than 2.44 wt.%. This may be attributed due to fact that as SH has many functional groups which have the ability to react with AAc and AM during polymerization process that could improve the polymeric network, and due to that the adsorption ability enhanced to a certain extent. However, on further increasing the SH content above 2.44 wt.%, it resulted in a decrease of adsorption capacity. This can be due to the fact that there are lots of –OH groups on the surface of SH, thus SH particles may act as cross-linking points in the polymeric network. As higher SH content could result in formation of more cross-link points, the elasticity of the polymeric chains decreased which in turn decreases the adsorption capacity of the superabsorbent hydrogel. Additionally, the amount of hydrophilic groups on the polymeric backbone decreased at higher SH content, which caused difficulty in the formation of an efficient adsorbent three-dimensional structure and thus decreased the adsorption capacity.

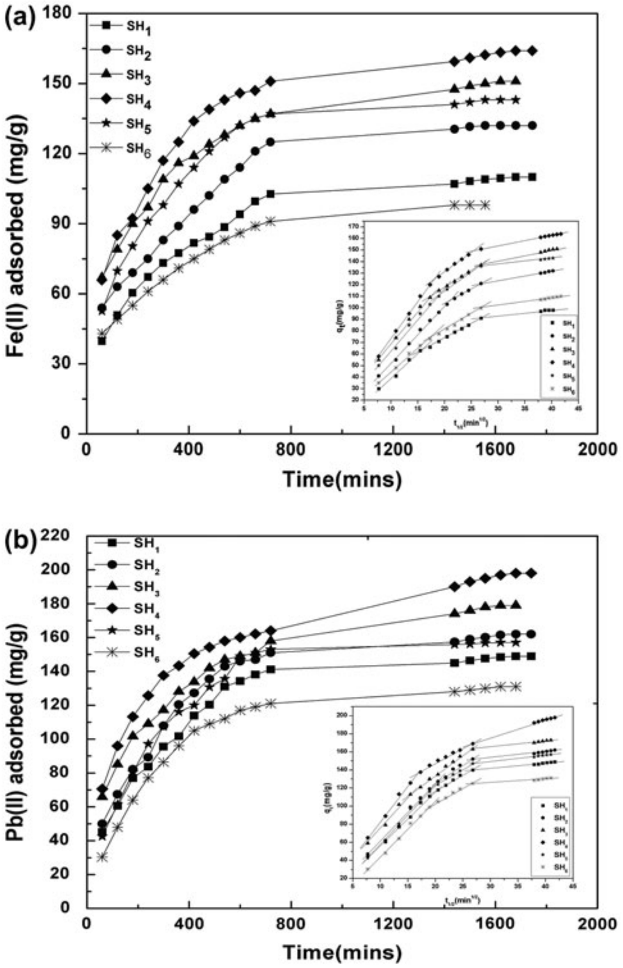

Fig. 7. (a) Effect of SH concentration on the adsorption of Pb^{2+}ions onto poly(AAc-SA-AM)/SH superabsorbent hydrogel with different concentrations of SH, inset figure (intraparticle diffusion kinetic plot for the adsorption of Pb^{2+}ions.) (b). Effect of SH concentration on the adsorption of Fe^{2+}ions adsorption onto poly(AAc-SA-AM)/SH superabsorbent hydrogel with different concentration of SH. Inset figure (Intraparticle diffusion kinetic plot for the adsorption of Fe^{2+}ions.) contact time, 48 h; initial ion concentration, 1,000 mg/L; temperature 30 ± 0.5℃; and hydrogel content, 50 mg.

3.6. Adsorption kinetics

Different kinetic models were cited to evaluate the experimental data obtained. Lagergren pseudo-first-order [23] and Ho and McKay's pseudo-second-order kinetic models [24] are two widely used models applied for solid–liquid adsorption.

Lagergren pseudo-first-order kinetic equation is given by:

$$\log(q_{1e} - q_t) = \log q_{1e} - k_1 t/2.303 \tag{7}$$

The equation may also be expressed as:

$$q_t = q_{1e}[1\,\exp(-k_1 t)] \tag{8}$$

Pseudo-second-order kinetic equation for equilibrium dye adsorption is given by:

$$t/q_t = 1/(k_2 q_2 e^2) + t/q_2 e \tag{9}$$

The equation can also be written as:

$$q_t = \frac{q_e^2 k_2 t}{1 + q_e k_2 t} \tag{10}$$

where q_{1e}, q_{2e}, and q_t (mg/g) represent the amount of metal ions adsorbed per unit mass of hydrogel at equilibrium and at any time t, respectively. The parameter k_1 (1/min) is the rate constant of the pseudo-first-order model and k_2 (g/(mg min)) is the rate constant of the pseudo-second-order model. The parameters k_1 and q_{1e} can be obtained from the slope and intercept of the plot of log $(q_{1e} - q_t)$ vs. t or by nonlinear fitting of q_t against t using Eq. (8). In the same way, the slope and intercept of the linear plot of t/q_t against t (Eq. (9)) or nonlinear fitting of q_t against t (Eq. (10)) gives the values of q_{2e} and k_2. The initial adsorption rate r_{id} (mg/g/min) can be calculated using the equation of $r_{id} = k_2\ q_{2e}^2$. The experimental data analyzed by the above two kinetic models and the parameters evaluated from given equations together with correlation coefficients are listed in Table 2.

It was observed from Table 2 that the linear correlation coefficients (R^2) for the pseudo-first-order kinetic model were obtained between 0.84 and 0.96 for Pb^{2+}ions and 0.91 to 0.98 for Fe^{2+}ions, respectively. In addition, there were large differences between the experimental q_e values ($q_{e,exp}$) and the calculated q_{1e} values of the pseudo-first-order model for both metal ions, which suggest that pseudo-first-order kinetic model does not fit well for the adsorption processes. It can also be found from Table 2 that linear correlation coefficients (R^2) for the pseudo-second-order kinetic model for all the hydrogels studied are over 0.98, which indicate that the pseudo-second-order model can be used for the whole adsorption process. Moreover, the q_{2e} values for the pseudo-second-order kinetic model were in perfect agreement with the $q_{e,exp}$ values. The results suggest that the pseudo-second-order adsorption model describes well the adsorption process, meaning that the adsorption rates of both ions onto the adsorbents are probably controlled by the chemical process.

Table 2
Estimated adsorption kinetic parameters for the adsorption of Pb^{2+}ions and Fe^{2+}ions on poly(AAc-SA-AM)/SH hydrogel in aqueous solutions

	Sample	Pseudo-first-order model				Pseudo-second-order model				Elovich model			Intraparticle diffusion model				
		q_e exp (mg/g)	q_{1e} cal (mg/g) Linear/nonlinear	$k_1 \times 10^3$ (min) Linear/nonlinear	R^2 Linear/nonlinear	q_{2e} cal (mg/g) Linear/nonlinear	$k_2 \times 10^5$ (g/mg min) Linear/nonlinear	r_{id} (mg/g/min) Linear/nonlinear	R^2 Linear/nonlinear	α (mg min/g)	β (g/mg) x10^3	R^2	k_1 (mg/g/min)	k_2 (mg/g/min)	k_3 (mg/g/min)	C	R^2
Pb^{2+} ion	SH_1	148.0	100.55/130	2.76/3.7	0.93/0.99	163.93/157	3.34/3.78	0.89/0.93	0.99/0.99	2.21	3.00	0.93	6.40	5.20	0.98	4.46	0.80
	SH_2	162.0	90.67/148	2.07/3.7	0.91/0.97	175.0/169	3.38/3.92	1.03/1.11	0.99/0.99	2.51	2.78	0.92	6.85	5.20	2.23	5.13	0.78
	SH_3	179.0	90.75/160	1.38/3.9	0.85/0.97	188.0/182	3.42/4.17	1.20/1.38	0.99/1.00	2.91	2.75	0.96	7.09	4.21	3.08	6.49	0.83
	SH_4	198.0	106.78/165	1.61/4.7	0.91/0.90	208.0/185	3.57/4.32	1.54/1.47	0.99/0.99	4.43	2.73	0.97	8.49	3.23	2.86	7.08	0.88
	SH_5	157.0	79.08/185	2.53/4.5	0.84/0.87	174.4/168	3.41/4.11	1.04/1.16	0.99/0.99	2.36	2.74	0.92	6.87	4.94	1.30	4.77	0.78
	SH_6	131.0	89.82/157	2.63/3.9	0.96/0.98	147.0/154	3.33/3.82	0.72/0.90	0.99/0.99	1.55	3.12	0.95	5.93	3.87	1.30	3.37	0.80
Fe^{2+} ion	SH_1	110.0	83.27/94.30	2.99/4.5	0.96/0.95	121.95/129	1.45/1.53	0.21/0.25	0.99/1.00	2.08	4.40	0.97	5.11	3.08	0.96	3.81	0.85
	SH_2	132.0	121.61/128	3.45/3.9	0.97/0.97	147.05/142	3.60/3.62	0.78/0.72	0.99/0.99	2.46	3.71	0.95	6.13	4.46	0.46	3.60	0.86
	SH_3	151.0	96.07/143	2.57/5.2	0.98/0.95	163.93/155	4.35/6.48	1.16/1.15	0.99/0.99	5.03	3.70	0.98	6.15	3.38	1.18	6.08	0.86
	SH_4	164.0	72.82/158	1.61/4.9	0.91/0.98	172.41/160	4.63/6.71	1.36/1.71	0.99/1.00	5.32	3.42	0.94	6.56	3.92	2.75	6.60	0.78
	SH_5	143.0	89.10/140	2.97/4.5	0.93/0.94	156.25/151	4.47/4.75	1.08/1.08	0.98/0.99	3.34	3.51	0.94	5.69	4.27	0.92	5.48	0.80
	SH_6	98.0	75.75/106	2.92/4.0	0.98/0.96	107.52/107	5.88/6.33	0.67/0.72	0.99/0.99	2.35	5.20	0.97	4.19	2.70	0.34	3.00	0.81

On comparing the correlation coefficients and calculated equilibrium adsorption capacities, q_{1e} and q_{2e} obtained by linear and nonlinear fitting of data, it is evident that nonlinear fitting provides better results Table 2: the values of R^2 are higher as compared to linear fit, while the difference between $q_{e,exp}$ and calculated q_e values are lower for the nonlinear fitting of both kinetic model.

The first- and second-order kinetic equations are based on the adsorption capacity. They only predict the adsorption behavior over the whole range of investigation on supporting the validity, as well as in agreement with chemisorption mechanism being the rate control.

Thus, these present findings remain uncertain for the adsorption mechanism. Therefore, the kinetic results were then analyzed by the Elovich equation and intraparticle diffusion mechanism.

Elovich equation was firstly applied for the kinetics of chemisorption of gases on solids and it has been successfully used for the adsorption of solute molecules from a liquid solution. The Elovich equation can be expressed as [25]:

$$q_t = (1/\beta)\ln(\alpha\beta) + (1/\beta)\ln t \tag{11}$$

where α is the initial adsorption rate (mg min/g), and the parameter β (g/mg) is related to activation energy for chemisorption. The values of the parameters (α, β), together with correlation coefficient are given in Table 2.

This model does not provide prediction about any definite mechanism, but it has been found useful in explaining chemical adsorption on highly heterogeneous surface. It can be observed from Table 2 that the regression coefficient for Elovich equation is lower than pseudo-first-order and pseudo-second-order equations.

Intraparticle diffusion mechanism can be expressed by equation [26]:

$$q_t = k_i t^{1/2} + C \tag{12}$$

where k_i (mg/g/min) is the intraparticle diffusion rate constant and C is a constant. The fitting of plot of q_t vs. $t^{1/2}$ for Pb^{2+} and Fe^{2+} ions are shown in inset Fig. 7(a) and (b), respectively. The values of constants k_i, C and the regression coefficient can be calculated from the slope of straight line portions of plot q_t vs. $t^{1/2}$.

The initial rates of intraparticle diffusion process were evaluated by linearization of the curve $q_{t=}t^{1/2}$. Previous study showed that such plot may present multilinearity [27]. It means two or more stages occur. The slope of each stage of curve is termed as the rate parameter $k_i (i = 1–3)$. Table 2 tabulates the rate parameters for all the hydrogel samples. The first rate for all the samples is higher compared to the second and the third stages, as this is an instantaneous adsorption stage. On the basis of above results, it can be concluded that in the whole adsorption process, three adsorption stages occurred. The first stage in the initial 3 h, the fast adsorption process, involves migration of the outer adsorption surface through film diffusion (through external mass transfer). The second stage, which is the gradual adsorption, the portion from 3 to 24 h, is the stage where both film diffusion and intra particle diffusion were operating simultaneously. The third one is the final equilibrium stage, where the film and intraparticle diffusion starts to slow down because of low solute concentration in sample solution.

From the Table 2, it can be clearly seen that the regression coefficient of intraparticle diffusion coefficient is lower in comparison to pseudo-first-order and pseudo-second-order kinetics, suggesting that adsorption of Pb^{2+}/Fe^{2+} ions did not follow intraparticle diffusion process. Nevertheless, the values of intercept were not zero, thus indicating that intraparticle diffusion mechanism cannot be the controlling factor for the kinetics of the adsorption process.

To evaluate the actual process involved in adsorption process, following equation can be employed [28]:

$$B_t = -\ln[1 - F] - 0.4799 \quad (13)$$

where B_t is a calculated mathematical function of F.

The linearity of plot B_t vs. t can be used to differentiate between the intraparticle diffusion and film diffusion mechanism. If the plot is a straight line passing through origin, the adsorption process will be governed by intraparticle diffusion and if not, then by film diffusion mechanism.

The plot is a straight line (with high linearity $R^2 > 0.998$), not passing through origin (figure not shown), and implies that Fe^{2+}/Pb^{2+} ions adsorption onto poly(AAc-SA-AM)/SH hydrogel was mainly regulated through the film diffusion mechanism with an important contribution of the intraparticle diffusion.

3.7. Effect of initial concentration of Pb^{2+}/ Fe^{2+} ions on adsorption capacity

Adsorption capacity of the poly(AAc-SA-AM)/SH hydrogel for the Pb^{2+}/Fe^{2+} ions as a function of different initial ion solution concentrations ranging from 200 to 1,200 mg/L is given in Fig. 8(a) and (b), respectively. As can be clearly seen from the Fig. 8(a) and (b), the amount of metal ions adsorbed on to the superabsorbent hydrogel increased with increase in initial concentration of metal ions solution, if the amount of adsorbent was kept unchanged. After obtaining a maximum at 1,000 mg/L, it levels off. From these plateau values, the maximum binding capacities for SH_4 hydrogel were found to be 198 and 164 mg/g/L for $Pb^{2+}$and Fe^{2+} ions, respectively. This can be explained as a fact of increase in the driving force of the concentration gradient with the high initial metal ions concentration. The initial metal ion concentration can provide the driving force to overcome the resistance to the mass transfer of metal ions between liquid and solid phases [29]. At a fixed adsorbent dose, the amount of removed metal ions increased with increasing concentration of solution and on the other hand, the percentage of adsorption

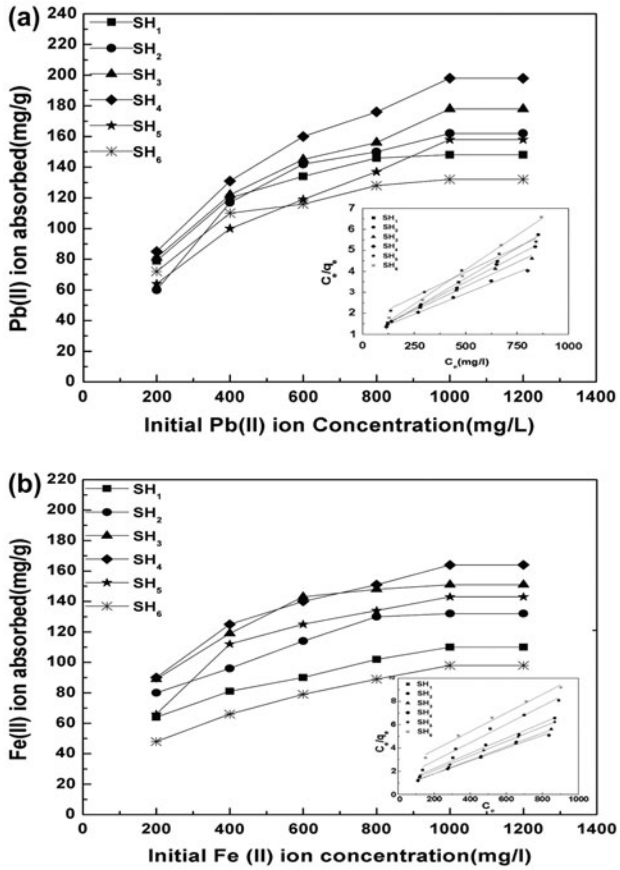

Fig. 8. Variation in the adsorption capacity as function of initial Pb^{2+}ions and Fe^{2+}ions concentration using poly (AAc-SA-AM)/SH superabsorbent hydrogel with different concentrations of SH. (a) Variation in the adsorption capacity as function of initial Pb^{2+}ions, inset figure (Langmuir adsoroption isotherm of Pb^{2+}ions adsorption) and (b) Variation in the adsorption capacity as function of initial Fe^{2+}ions concentration, inset figure (Langmuir adsoroption isotherm of Fe^{2+}ions adsorption.

decreased. In other words, for high initial metal ion concentration, the residual concentration of metal ions will be high. At low concentration, the ratio of initial number of metal ions to the available active sites is low and so the fractional adsorption becomes independent of initial concentration. In the case of higher concentration, however, the number of available active sites becomes lesser and subsequently the adsorption of metal ions depends on the initial concentration.

3.8. Adsorption Isotherms

Adsorption characteristics and equilibrium data, which are commonly known as adsorption isotherm, describe how the adsorbate interacts with adsorbent and so, isotherms are critical in optimizing the use of adsorbent. The adsorption experimental data are generally interpreted with the Langmuir, Freundlich, and Dubinin–Radushkevich (D–R) isotherm models.

The most widely used isotherm for the modeling of adsorption data is the Langmuir adsorption isotherm. The Langmuir adsorption isotherm equation may be described as [30,31]:

$$\frac{C_e}{q_e} = \frac{1}{K_e\, q_{\max}} + \frac{C_e}{q_{\max}} \tag{14}$$

The Freundlich model is an empirical equation and is applied to describe heterogeneous surface system described by a heterogeneity factor of *1/n*. This model is characterized by reversible adsorption and is not limited to the formation of the monolayer. The Freundlich model in linear form may be expressed as follows [32]:

$$\log(q_e) = 1/n \log(C_e) + \log K_f \tag{15}$$

where K_e is the sorption equilibrium constant (L/mg), $q_{\max}$ is themaximum amount of adsorption (mg/g), C_e is the equilibrium concentration of the metal ion in the solution (mg/L), and q_e the amount adsorbed at equilibrium mg/g. K_f (L/g) and *1/n* (dimensionless) are the Freundlich constants related to the adsorption capacity and the degree of heterogeneity, respectively. The Langmuir and Freundlich constants and regression coefficients were calculated from the linear plots of C_e/q_e vs. C_e and log (q_e) vs. log(C_e), respectively.

The D–R isotherm can be subjected to depict the nature of adsorption as a physical or chemical process on both homogeneous and heterogeneous surfaces [33]. A linear form of D–R equation is presented by the following relationship:

$$\ln q_e = \ln q_m - \beta \varepsilon^2 \tag{16}$$

where β is a constant correlated to mean free energy of adsorption ((mol/J)^2), q_m is the theoretical equilibrium capacity, and ε is the Polanyi potential, which is related to the equilibrium Pb^{2+}/ Fe^{2+} ions concentration (J/mol), illustrated as follows:

$$\varepsilon = RT \ln(1 + 1/C_e) \tag{17}$$

where R ((8.314 J/(mol K)) is the gas constant and T (K) is the absolute temperature. The D–R constant may give valuable information about the mean free energy, E (J/mol), which can be evaluated from constant β, [34] using the following equation:

$$E = (2\beta)^{0.5} \tag{18}$$

The constant parameters and regression coefficients obtained from Langmuir, Freundlich, and D–R adsorption equations mentioned above are summarized in Table 2.

The fit of the data for Pb^{2+}/Fe^{2+} ions adsorption suggest that the values of regression coefficients of Langmuir model were higher than those of Freundlich and D–R models, indicating that Langmuir isotherm model correctly fitted the equilibrium data. It should be mentioned that linearity obtained from Freundlich isotherm was quite poor with the regression coefficients lying between 0.8917–0.9792 for Pb^{2+} ions and 0.9006–0.9881 for Fe^{2+} ions, respectively during the whole concentration investigated.

The plots of Langmuir adsorption isotherm of Pb^{2+} and Fe^{2+} ions are shown in inset Fig. 8(a) and (b), respectively. The plots give straight line over the whole concentration range studied. The q_{max} values of the SAHs obtained by Langmuir equation were quite consistent with the experimental one (Table 3). The applicability of Langmuir isotherm model and higher values of correlation coefficient (R^2 value found in the range of 0.9813–0.9985 and 0.9891–0.9997 for Pb^{2+} ions and Fe^{2+} ions, respectively) suggest a favorable and monolayer adsorption. It can be concluded that the adsorption behavior for Pb^{2+} and Fe^{2+} ions can be satisfactorily explained by Langmuir adsorption isotherm.

The values of mean free adsorption energy (E) evaluated from the D–R adsorption model are listed in Table 3. When one mole of ions is transferred, value of E in the range of 1–8 kJ mol^{-1} suggests physical adsorption, while the value of E is between 8 and 16 kJ mol^{-1} indicates that adsorption process occur by ion exchange. The E value was higher than 8.0 kJ/mol, although the values of R^2 was less than 0.9, meaning that adsorption rates of Pb^{2+}/Fe^{2+} ions onto poly

Table 3
Estimated adsorption isotherm parameters for the adsorption of Pb^{2+}ions and Fe^{2+}ions on poly(AAc-SA-AM)/SH hydrogel in aqueous solutions

	Sample designation	Langmuir model				Freundlich model			D-R equation	
		q_e (mg/g)	q_{max} (mg/g)	$K_e \times 10^3$ (L/mg)	R^2	K_f (mg/g)	n	R^2	E	R^2
Pb^{2+}	SH_1	148.0	172.4	7.38	0.99	9.3	1.86	0.96	24.26	0.63
	SH_2	162.0	196.0	5.57	0.99	4.7	1.85	0.90	17.49	0.74
	SH_3	179.0	217.0	4.70	0.98	9.1	2.28	0.89	17.14	0.59
	SH_4	198.0	250.0	4.10	0.99	9.4	2.19	0.96	16.80	0.84
	SH_5	157.0	208.3	4.26	0.99	4.1	1.87	0.89	20.95	0.87
	SH_6	131.0	151.0	8.35	0.99	3.6	1.82	0.97	21.49	0.78
Fe^{2+}	SH_1	110.0	126.5	10.0	0.99	11.1	3.75	0.90	18.87	0.98
	SH_2	132.0	151.5	9.63	0.99	18.3	3.40	0.98	17.00	0.96
	SH_3	151.0	172.4	9.37	0.99	21.2	3.34	0.95	16.90	0.76
	SH_4	164.0	181.8	7.75	0.99	24.7	3.57	0.97	14.17	0.75
	SH_5	143.0	158.3	7.84	0.99	11.4	2.59	0.92	16.71	0.91
	SH_6	98.0	123.7	9.98	0.99	5.87	2.39	0.98	22.02	0.85

(AAc-SA-AM)/SH hydrogel is probably controlled by the chemical process.

3.9. Effect of temperature on the adsorption

Temperature is one of the important parameters that influence the adsorption capacity of adsorbents. Fig. 9(a) shows the influence of temperature on adsorption capacity of Pb^{2+} and Fe^{2+} ions onto poly (AAc-SA-AM)/SH hydrogel surface. It was observed from the figure that with increasing temperature from 20 to 30℃, the adsorption amount of both ions increased (for Pb^{2+} ions, from 167 to 198 mg/g and for Fe^{2+} ions, from 141 to 164 mg/g, respectively). However, with further increase in temperature from 30 to 60℃, the adsorption capacity of poly(AAc-SA-AM)/SH for Pb^{2+} and Fe^{2+} ions decreases. Adsorption is a dynamic process, and it involves both adsorption and desorption phenomenon. The adsorbates are attracted by the surface force and attach to the surface of the adsorbent. The adsorbate molecules are in constant motion also. The increment in temperature increases the energy of adsorbed molecules. The high energy then speeds up the Brownian motion, and thus requires a stronger force to keep the adsorbed molecules attached onto the adsorbent surface (the higher the adsorption process temperature, higher the speed of the adsorbate molecules' Brownian motion, resulting in reduction in the possibility of adsorption amount of the adsorbate molecules). At the high temperature, the adsorbed molecules have enough energy to overcome the attraction force and to migrate back from the solid phase to bulk phase. Another reason is the presence of lesser number of active binding sites at higher temperature [35] that may be attributed due to the deactivation of the surface of adsorbent or due to destruction of some active binding sites existing on the adsorbent surface because of bond rupture. This result can also confirm the exothermic nature of adsorption for both ions onto adsorbent surfaces. So, 303 K was chosen as the solution temperature. Similar type of nature has also been observed for the adsorption of other metals [36].

3.10. Thermodynamic parameters of adsorption

Thermodynamic parameters, including Gibbs free energy change (ΔG), standard enthalpy change (ΔH), and standard entropy change (ΔS), are the actual indicators for the practical application of an adsorption process. On the basis of nature of Gibbs free energy change (whether it is positive or negative), the spontaneous nature of adsorption may be determined. According to values of these thermodynamic parameters, whether the process will occur spontaneously may be determined. In the present case, these thermodynamic parameters were calculated for the SH_4 hydrogel. The Gibbs free energy change for any reaction may be expressed as follows: [37];

$$\Delta G = \Delta G^\circ + RT \ln K_e \tag{19}$$

When the adsorption reaches the equilibrium state, ΔG becomes zero, and so ΔG° is equal to $-RT \ln K_e$, where K_e represents the equilibrium constant, R is the universal gas constant (8.314 $\mathrm{Jmol^{-1}\,K^{-1}}$), and T is temperature in Kelvin.

The temperature dependence of the Gibbs free energy change may be given by the following equation [38]:

$$d(\Delta G^\circ/T) = -\Delta H^\circ/T^2 dt \tag{20}$$

$$\ln K_e = -(\Delta H^\circ/R)(1/T) + \Delta S^\circ/R \tag{21}$$

The thermodynamic equilibrium constant may be expressed in terms of enthalpy change of adsorption reaction as a function of temperature. Assuming that standard enthalpy change (ΔH°) is approximately independent of temperature, the slope of the plot of $\ln K_e$ vs. $1/T$ is equal to $-\Delta H^\circ/R$. The standard adsorption entropy change can be determined from the equation as

$$\Delta S^\circ = (\Delta H^\circ - \Delta G^\circ)/T \tag{22}$$

Inset Fig. 9(a) represents the plots of $\ln K_e$ vs. $1/T$. Changes in ΔS° and ΔG° should be considered to determine whether the process is spontaneous. The Gibbs free energy change indicates the spontaneous nature of the adsorption process and higher negative value shows a more energetically favorable adsorption [39]. The results of experiments are summarized in Table 4.

The equilibrium constants determined from Langmuir equation at 303.15, 318.15, and 333.15 Kelvin were used to evaluate these thermodynamic parameters of the adsorption. The negative values for standard enthalpy change suggest that the adsorptions of both ions are exothermic, which is evidenced by the decrement in the adsorption of both ions with increase in the temperature. A negative change in ΔG° indicates that the adsorption process is spontaneous [40,41], further, with the increasing temperature, the decrease in the values of ΔG° indicates that the adsorption reaction was more spontaneous at higher temperatures. The positive value for entropy change reveals the increase in randomness at the solid–solution interface at the time of the adsorption of Pb^{2+}/Fe^{2+} ions on the adsorbent.

3.11. Effect of ionic strength on adsorption

There are several metal ions such as K^+ and Na^+ present in the wastewater, and the existence of these ions may either accelerate or retard the adsorption of metal ions by adsorbents. Accordingly, effect of ionic strength on the adsorption of Pb^{2+} ions and Fe^{2+} ions onto SH_4 hydrogel at different concentrations of potassium nitrate and sodium chloride was investigated, as shown in Fig. 9(b). It is clear that when the KNO_3/NaCl concentration is below 10 mmol/L, the adsorption capacity of poly(AAc-SA-AM)/SH hydrogel is observed to decrease a little in comparison to that in distilled water. Further increasing the concentration KNO_3/NaCl would result in an appreciable decrease in the adsorption amount. This is attributed to fact that the counter ions compete with the cations on the active sites and would neutralize the negatively charged groups, thereby disabling poly(AAc-SA-AM)/SH hydrogel to interact with the cationic adsorbate. So, the increase of ionic strength would reduce the uptake capacity of Pb^{2+}/Fe^{2+} ions.

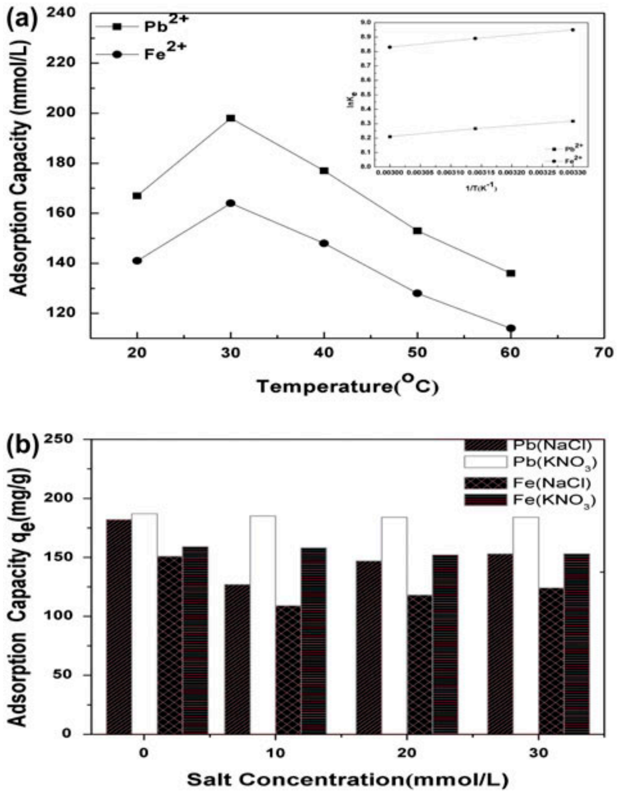

Fig. 9. Effect of temperature and ionic strength on the adsorption of Pb^{2+}ions and Fe^{2+}ions onto SH_4 superabsorbent hydrogel. (a) Effect of temperature, inset figure (plot of $\ln K_e$ vs. T^{-1} for the evaluation of thermodynamic parameters of the phosphate ion adsorption process) (b) Effect of ionic strength.

3.12. Comparison with other alternative adsorbents

When the equilibrium adsorption of Pb^{2+}/Fe^{2+} ions of our SH_4 hydrogel was compared with the work of

Table 4
Thermodynamic parameters for adsorption of Pb^{2+}ions and Fe^{2+}ions on poly(AAc-SA-AM)/SH hydrogel (SH_4) at various temperatures

T(K)	Pb^{++} ion				Fe^{++} ion			
	$K_e \times 10^3$	ΔG° (kJ/mol)	ΔH° (kJ/mol)	ΔS° (J/molK)	$K_e \times 10^3$	ΔG° (kJ/mol)	ΔH° (kJ/mol)	ΔS° (J/molK)
303.15	4.10	−20.96	−2.98	59.30	7.75	−22.40	−3.320	62.95
318.15	3.89	−21.86		59.33	7.24	−23.51		63.46
333.15	3.68	−22.05		58.99	6.91	−23.72		63.12

Table 5
Comparison table for removal capacities (q_e) of Pb^{2+}ions and Fe^{2+}ions by various adsorbents

Pb^{++} ion			Fe^{++} ion		
Absorbent	q_e (mg/g)	Ref.	Absorbent	q_e (mg/g)	Ref.
Carbon aerogel	34.72	[42]	Cell-CN-cl-poly(AAm)	10.64	[46]
Hydroxyapatite/polyacrylamide	178.00	[43]	*N*-vinylpyrrolidone /acrylic acid/ 2-acrylamido-2-methylpropane sulphonicacid	40.9	[47]
Poly(acrylamide-co-sodium methacrylate)	68.90	[44]	PVP/AAc	36	[48]
Magnetic poly (2-acrylamido-2-methyl-1-propanesulfonic acid)	140.84	[45]	Hydroxypropyl cellulose (HPC)	19	[49]
poly(AAc-SA-AM)/SH hydrogel	198	This work	poly(AAc-SA-AM)/SH hydrogel	164	This work

other researchers (shown in Table 5) [42–49], it was evident that the synthesized poly(AAc-SA-AM)/SH hydrogel has high adsorption capacity of 198 and 164 mg/g for $Pb^{2+}$and Fe^{2+} ions, respectively, indicating that the adsorbent described in the present study represents better values and higher affinity towards the effective adsorption of metal ions under study. Thus, poly(AAc-SA-AM)/SH hydrogel can be effectively and economically used as wastewater purifier.

3.13. Desorption/regeneration of adsorbent

A good solid adsorbent in addition to its high adsorption ability must also exhibit a good regeneration capacity for multiple uses. The recovery of metal ions is an important parameter characterizing the economics of the process. Desorption studies can help to recover the Pb^{2+}/Fe^{2+} ions from the adsorbent and regenerate the superabsorbent hydrogel, so that it can be used again and again. Desorption of Pb^{2+}/ Fe^{2+} ions were also studied in a batch experimental setup. The poly(AAc-SA-AM)/SH hydrogel used for the adsorption of Pb^{2+}/ Fe^{2+} ions was placed in elution medium for 24 h and the amount of Pb^{2+}/ Fe^{2+} ions desorbed to the elution medium was measured. Table 1 shows the relationship between the adsorption capacity and times of reuse for the sample. So after several times of reuse, the adsorption capacity of superabsorbent hydrogel decreases only slightly compared to initial one. Thus, it can be concluded that the poly(AAc-SA-AM)/SH hydrogel showed stable Pb^{2+}/Fe^{2+} ions removal capacities after repeated regeneration.

4. Conclusion

The study showed that both metals, i.e. lead and iron were removed more effectively and in high quantities from aqueous solutions as compared to other commonly used adsorbents (such as carbon aerogel, acrylic acid or acrylamide, and sulfonic acid derivative-based hydrogels) using poly(AAc-SA-AM)/SH hydrogel as adsorption agent. Batch adsorption experiments were carried out at different conditions including time, pH, SH concentration, temperature, ionic strength, and concentration of the metal ions to investigate the optimum values of the above-mentioned parameters. The results revealed that poly(AAc-SA-AM)/SH hydrogel adsorbs both ions better than poly (AAc-SA-AM) hydrogel and the maximum adsorption capacity was obtained when 2.44 wt.% SH was used (for Pb^{2+} ions 198 mg/g and164 mg/g for Fe^{2+} ions; initial concentration 1,000 mg/L). It was also found that pH 5.5 and 2.5 is the best pH to achieve the maximum adsorption of Pb^{2+} and Fe^{2+} ions, respectively, and also the optimum temperature was found to be 303.15 K. The adsorption isotherms for Pb^{2+} ions and Fe^{2+} ions agree well with the Langmuir model. The adsorption process of Pb^{2+} and Fe^{2+} ions onto poly (AAc-SA-AM)/SH hydrogel is exothermic and spontaneous, and follows the pseudo-second-order kinetics.

The results of five-time consecutive adsorption–desorption cycle show that the poly(AAc-SA-AM)/SH hydrogel has high adsorption and desorption efficiency, which indicates that it can be used as an effective solid adsorbent for the removal of metal ions from wastewater and aqueous effluents.

Acknowledgment

This work was financially supported by the University Grant Commission New Delhi, India (39-875-2010).

Nomenclature

q_{1e}, q_{2e}, — amount of phosphate ions adsorbed at equilibrium (mg/g)
C_o — initial concentration of metal ions (mg/L)
C_e — equilibrium concentration of the metal ion in the solution (mg/L)
V — volume of the metal ions solution (L)
M — mass of hydrogel sample (g)
K_e — adsorption equilibrium constant (Lmg^{-1})
q_{max} — maximum amount of adsorption (mg/g)
K_f — Freundlich constants related to the adsorption capacity (mg/g)
N — Freundlich constants related to degree of heterogeneity
ΔG — Gibbs free energy change (kJ/mol)
ΔH — standard enthalpy change (kJ/mol)
ΔS — standard entropy change (J/mol K)
R — universal gas constant ($Jmol^{-1}$ K^{-1})
T — temperature (Kelvin)
q_t — asorption capacities at any time t (mg/g)
k_1 — rate constant of the pseudo-first-order model (min^{-1})
k_2 — rate constant of the pseudo-second-order model (g/(mg min)

References

[1] Agency for toxic substances and Disease Registry (ATSDR), Toxicological, Profile for Phenol. U S department of Health and Human services, Bethesda, MD, 1998.

[2] A. Oliva, A. Molinari, F. Zuniga, P. Ponce, Studies on the liquid–liquid extraction of nickel(II), zinc (II), cadmium (II), mercury (II) and lead (II) with 1-phenyl-3-hydroxy-4- dodecyldithiocarboxylate-5-pyrazolone Removing heavy metals from waste water, Microchim. Acta. 140 (2002) 201–210.

[3] A. Demirbas, Heavy metal adsorption onto agro-based waste materials: A review, J. Hazard. Mater. 157 (2008) 220–229.

[4] S.S. Ahluwalia, D. Goyal, Microbial and plant derived biomass for removal of heavy metals from wastewater, Bioresour. Technol. 98 (2007) 2243–2257.

[5] V.M. Nurchi, I. Villaescusa, Agricultural biomasses as sorbents of some trace metals, Biotechnol. Bioeng. 42 (2008) 785–787.

[6] P.A. Brown, S.A. Gill, S.J. Allen, Metal removal from wastewater using peat, Water Res. 34 (2000) 3907–3916.

[7] K. Kosemund, H. Schlatter, J.L. Ochsenhirt, E.L. Krause, D.S. Marsman, G.N. Erasala, Saftey evaluation of superabsorbent baby diapers Regulatory, Toxicol. Pharmacol. 53 (2009) 81–89.

[8] L.C. Dong, A.S. Hoffman, A novel approach for preparation of pH- sensitive hydrogels for enteric drug delivery, J. Controlled Release 15 (1991) 141–152.

[9] K.B. Sunil, S. Surinderpal, Analysis of swelling behavior of poly(methacrylamide-co-methacrylic acid) hydrogels and effect of synthesis conditions on water uptake, React. Funct. Polym. 66 (2006) 431–440.

[10] E. Karadag, D. Saraydin, Y. Caldiran, O. Guven, Swelling studies of copolymeric acrylamide/crotonic acid hydrogels as carriers for agricultural uses, Polym. Adv. Technol. 11 (2000) 59–60.

[11] C.O. Walker, U.S. Pat. 4 (1987) 664–665.

[12] P.S. Keshava Murthy, Murali Mohan, J. Sreeramulu, K. Mohana Raju, Semi-IPNs of starch and poly(acrylamide-co-sodium methacrylate): Preparation, swelling and diffusion characteristics evaluation, React. Funct. Polym. 66 (2006) 1482–1493.

[13] K. Kabiri, H. Omidian, S.A. Hashemi, M.J. Zohuriaan-Mehr, Synthesis of fast-swelling superabsorbent hydrogels: Effect of crosslinker type and concentration on porosity and absorption rate, Eur. Polym. J. 39 (2003) 1341–1348.

[14] N. Sahiner, Hydrogel nanonetworks with functional core-shell structure, Eur. Polym. J. 43 (2007) 1709–1717.

[15] A.S. Hoffman, Hydrogels for biomedical applications, Adv. Drug Deliv. Rev. 43 (2002) 3–12.

[16] W. Wang, A. Wang, Synthesis, swelling behaviors, and slow-release characteristics of a guar gum-g-poly(sodium acrylate)/sodium humate superabsorbent, J. Appl. Polym. Sci. 112 (2009) 2102–2111.

[17] J. Liu, Q. Wang, A. Wang, Synthesis and characterization of chitosan-g-poly(acrylic acid)/sodium humate Superabsorbent, Carbohydr. Polym. 70 (2007) 166–173.

[18] W. Li, H. Zhao, P. Teasdale, R. John, Preparation and characterisation of a poly(acrylamidoglycolic acid-co-acrylamide) hydrogel for selective binding of Cu^{2+} and application to diffusive gradients in thin films measurements, React. Funct. Polym. 43 (2002) 4803–4809.

[19] J. Hizal, R. Apak, Modeling of cadmium(II) adsorption on kaolinite-based clays in the absence and presence of humic acid, Appl. Clay Sci. 32 (2006) 232–244.

[20] J.Z. Yi, Y.Q. Ma, L.M. Zhang, Synthesis and decoloring properties of sodium humate/poly (N-isopropylacrylamide) hydrogels, Bioresour. Technol. 99 (2008) 5362–5367.

[21] S.M. Lee, A.P. Davis, Removal of Cu(II) and Cd(II) from aqueous solution by seafood processing waste sludge, Water Res. 35 (2001) 534–540.

[22] K.A. Dashkhuu, Y.G. Ko, U.S. Choi, Adsorption and equilibrium adsorption modeling of bivalent metal cations on viscose rayon succinate at different pHs, React. Funct. Polym. 67 (2007) 312–318.

[23] S. Lagergren, K.S. Vetenskapsakademiens, Zur theorie der sogenannten adsorption geloster stoffe [About the theory of so called adsorption of soluble subtances], Handlingar 24 (1898) 1–39.

[24] Y.S. Ho, G. McKay, Pseudo-second order model for adsorption processes, Process Biochem. 34 (1999) 451–465.

[25] H.A. Taylor, N. Thon, Kinetics of Chemisorption, J. Am. Chem. Soc. 74 (1952) 4169–4173.

[26] J. Weber, J.C. Morris, Kinetic of adsorption on carbon solution, J. Sanitery Eng. Div. Am. Soc. Civ. Eng. 89 (1963) 31–60.

[27] C.W. Feng, L.T. Ru, S.J. Ruey, Comparative adsorption of metal and dye on flake and bead-types of chitosans prepared from fishery wastes, J. Hazard Mater. 73 (2000) 63–75.

[28] D. Reichenberg, Properties of ion-exchange resins in relation to their structure III, kinetics of exchange, J. Am. Chem. Soc. 75 (1953) 589–597.

[29] V.C. Srivastava, M.M. Swamy, I.D. Mall, B. Prasad, I.M. Mishra, Adsorptive removal of phenol by bagasse fly ash and activated carbon: Equilibrium, kinetics and thermodynamics, Colloids Surf., A 272 (2006) 89–104.

[30] I.J. Langmuir, The adsorption of gases on plane surfaces of glass, mica and platinum, J Am. Chem. Soc. 40 (1918) 1361–1368.

[31] Y.S. Ho, C.T. Huang, H.W. Huang, Equilibrium sorption isotherm for metal ions on tree fern, Process Biochem. 37 (2002) 1421–1430.

[32] M. Jaroniec, Physical adsorption on heterogeneous solids, Adv. Colloid Interface Sci. 18 (1983) 149–225.

[33] T. Shahwan, H.N. Erten, Temperature effects in barium sorption on natural kaolinite and chlorite-illite clays, J. Radioanal. Nucl. Chem 260 (2004) 43–48.

[34] J.P. Hobson, Physical adsorption isotherms extending from ultrahigh vacuum to vapor pressure, J. Phy. Chem. 73 (1969) 2720–2727.

[35] M.S. Berber, R.L. Mendoza, P.A. Ramos, J. Davila, P.E. Mendoza, J. Flores, Comparison of isotherms for the ion Exchange of Pb(II) from Aqueous Solution onto homoionic clinoptilolite, J. Colloid Interface Sci. 301 (2006) 40–45.

[36] Z. Reddad, C. Gerente, Y. Andres, J.F. Thibault, P. Le Cloirec, Cadmium and lead adsorption by natural polysaccharide in MF membrane reactor: Experimental analysis and modeling, Water Res. 37 (2003) 3983–3991.

[37] Y. Liu, Some consideration on the Langmuir isotherm equation, Colloids Surf., A 274 (2006) 34–36.

[38] M. Alkan, O. Demirbas, S. Elikcapa, M. Dogan, Sorption of acid red 57 from aqueous solution onto sepiolite, J. Hazard. Mater. 116 (2004) 135–145.

[39] K.S. Walton, J. Cavalcante, M.D. LeVan, Adsorption of light alkanes on coconut nanoporous activated carbon, Braz. J. Chem. Eng. 23 (2006) 555–561.

[40] J.M. Smith, H.C. Van Ness, Introduction to Chemical Engineering Thermodynamics, fourth ed, McGraw-Hill, Red Lion, PA, 1987.

[41] D. Do, Adsorption Analysis: Equilibria and Kinetics, Imperial College Press, London, 1998.

[42] K. Kadirvelu, J. Goel, C.J. Rajagopal, Sorption of lead, mercury and cadmium ions in multi-component system using carbon aerogel as adsorbent, J. Hazard. Mater. 153 (2008) 502–507.

[43] S.H. Jang, Y.G. Jeong, B.G. Min, W.S. Lyoo, S.C. Lee, Preparation and lead ion removal property of hydroxyapatite/polyacrylamide composite hydrogels, J. Hazard. Mater. 159 (2008) 294–299.

[44] M.K. Krušić, N. Milosavljević, A. Debeljković, Ö.B. Üzüm, E. Karadağ, Removal of Pb^{2+} ions from water by poly(acrylamide-co-sodium methacrylate) hydrogels, Water Air Soil Pollut. 223 (2012) 4355–4368.

[45] O. Ozay, S. Ekici, Y. Baran, N. Aktas, N. Sahiner, Removal of toxic metal ions with magnetic hydrogels, Water Res. 43 (2007) 5114–5119.

[46] G.S. Chauhan, B. Singh, S. Chauhan, M. Verma, S. Mahajan, Sorption of some metal ions on cellulosic-based hydrogels, Desalination 181 (2005) 217–224.

[47] E.K. Yetimoglu, M.V. Kahraman, O. Ercan, Z.S. Akdemir, N. K. Apohan, N-vinylpyrrolidone/acrylic acid/2-acrylamido-2-methylpropane sulfonic acid based hydrogels: Synthesis, characterization and their application in the removal of heavy metals, React. Funct. Polym. 67 (2007) 451–460.

[48] E.H. Ali, H.A. Shawky, H.A. Rehim, E.A. Hegazy, Synthesis and characterization of PVP/AAc copolymer hydrogel and its applications in the removal of heavy metals from aqueous solution, Eur. Polym. J. 39 (2003) 2337–2344.

[49] G.S. Chauhan, S. Mahajan, Use of novel hydrogels based on modified cellulosics and methacrylamide for separation of metal ions from water systems, J. Appl. Polym. Sci. 86 (2002) 667–671.